Band-gap narrowing in GaAs using a capacitance method

P. Van Mieghem, R. P. Mertens, G. Borghs, and R. J. Van Overstraeten
Interuniversity Micro-Electronics Center, Kapeldreef 75, B-3030 Leuven, Belgium
(Received 13 September 1989)

Since the precise value of band-gap narrowing is difficult to determine, many values have been reported in the literature. Optical methods have been considered to yield the most accurate values. Here we present the results of capacitance measurements on abrupt GaAs diodes carried out at various temperatures. The value of band-gap narrowing is derived with use of a new formalism. The agreement between the values of band-gap narrowing obtained by this method and by optical methods is good, demonstrating the validity of the applied theory. In contrast with other electrical measurements, this method does not require the knowledge of material parameters such as mobility, lifetime, and diffusion constants, which are difficult to estimate.

I. INTRODUCTION

In GaAs, little experimental effort has been devoted to study band-gap narrowing (BGN), due to heavy doping, by electrical methods. Mainly optical methods such as photoluminescence (PL),[1] cathodoluminescence,[2] and optical diode measurements[3] have been used. In silicon , on the contrary, electrical methods[4] that interpret the *pn* product have been applied, but more recently these have been criticized.[5–7] The fundamental arguments against these methods are the obvious shortcoming of the Boltzmann *np*-product formula which is employed in situations where Fermi-Dirac statistics should be applied and the empirical derivation of an effective band gap from electrical current-voltage measurements whose relationship to the real shrinkage of the band gap is far from being clear today. Besides the lack of theoretical rigor, a relatively large number of parameters such as mobility, lifetime, and diffusion constant, which are difficult to measure, must be determined. As pointed out by Del Alamo,[7] about 1 order of magnitude of disagreement in the determination of parameters such as lifetime and mobility is found among the various authors and this has caused a confusing situation in the reported BGN data. Moreover, Del Alamo shows that at least two independent measurements (a dc and an ac) are needed to extract BGN information from current measurements.

Here we present data of BGN in GaAs using an electrical method.[8] The method was first proposed by Van Overstraeten *et al.*[9] and is based on a capacitance measurement of an abrupt symmetrically doped diode. This capacitance method is superior to current-voltage measurements methods mentioned above and in Ref. 10; since no additional measurements are necessary, the measurement technique is relatively simple and no material parameters (as mobility, lifetime, and diffusion constants) are involved.

Lowney[11] used a similar technique for linearly graded Si junctions with heavily doped and compensated *p* and *n* sides. He interpreted the effective BGN as the difference between the theoretical intercept voltage of Chawla and Gummel[12] and the observed intercept voltage. As an explanation for the discrepancy between his results and previous published ones, he proposed a screening effect of the ions in the space-charge region. However, since there exists no analytical formula for the intercept voltage for linearly graded junctions, there are no simple reasons to conclude that any difference between the measured and the Chawla-Gummel intercept voltage equals BGN. On the other hand, for an abrupt junction with constant symmetrical doping levels, an analytically accurate formula for the intercept voltage is presented in Sec. II.

In the third section, we discuss the choice of the density-of-states (DOS) functions. The experimental values of the intercept voltage of abrupt GaAs diodes are reported in Sec. IV. The last section compares the experimental results obtained by the present method with optical results.

II. THEORY

If the inverse capacitance squared (C^{-2}) of an abrupt *n-p* junction is plotted versus applied voltage (V) across the junction, the data points are theoretically expected to lie on a straight line under low injection conditions. Hence, in that regime, the $C^{-2}(V)$ function is unambiguously determined by two independent quantities, most often the slope and the intercept voltage (V_{int}). The slope of the straight line is related to the effective doping concentration (N_{eff}) of the diode,

$$N_{\text{eff}}=\frac{2N_A N_D}{N_A+N_D} \tag{2.1}$$

while the intercept voltage is a function of the band gap and the doping concentration of both *n*- and *p*-type regions.

Since this capacitance method basically reflects the behavior of the majority carriers, the extracted value of the band-gap shrinkage consists of the two contributions due to the majority carriers, the lowering of the conduction band in the *n*-type region ΔE_c^n and the upward shift of the valence band in the *p*-type region ΔE_v^p. Theoretical calculations[3] show that the self-energies around the Fer-

mi level for the valence and conduction band are almost equal, or

$$\Delta E_c^{n\ (p)} \approx \Delta E_v^{n\ (p)} . \tag{2.2}$$

Hence,

$$\Delta E_c^n + \Delta E_v^p \approx \Delta \left[\frac{E_{gn} + E_{gp}}{2} \right] \equiv \Delta E_{g\ \mathrm{av}} , \tag{2.3}$$

where E_{gn} (E_{gp}) denotes the band gap of the n-type (p-type) material and Δ expresses the narrowing. The theory[3] and the good agreement with optical measurements justifies the concept of the average band gap $E_{g\ \mathrm{av}}$ (further expressed in meV).

Generally, the classical formula,[13] which we call the Boltzmann intercept voltage formula (2.4), is used to determine the band gap of an abrupt symmetrically doped [$N_D = N_A = N$ and, from (2.1), $N_{\mathrm{eff}} = N$] diode,

$$V_{\mathrm{int}} = E_{g\ \mathrm{av}} + \frac{kT}{q} \left[\ln \left[\frac{N}{N_c} \right] + \ln \left[\frac{N}{N_v} \right] - 2 \right] , \tag{2.4}$$

where N_c (N_v) is the effective DOS in the conduction (valence) band. However, for low temperatures or heavily doped semiconductors, the Boltzmann statistics are not valid anymore and must be replaced by the Fermi-Dirac statistics. This suggests a modification of (2.4), which we call the Fermi intercept voltage formula (2.5),

$$V_{\mathrm{int}} = E_{g\ \mathrm{av}} + \frac{kT}{q} [F_{1/2}^{-1}(N/N_c) + F_{1/2}^{-1}(N/N_v) - 2] , \tag{2.5}$$

where $F_{1/2}^{-1}(x)$ is the inverse of the Fermi-Dirac integral of the order one-half. However, expression (2.5) is logically inconsistent, and as shown in Appendix A the correct formula (2.6) should be used:

$$V_{\mathrm{int}} = E_{g\ \mathrm{av}} + \frac{kT}{q} [F_{1/2}^{-1}(N/N_c) + F_{1/2}^{-1}(N/N_v) - Z(N)] \tag{2.6}$$

and $Z(N)$, plotted in Fig. 1, equals

$$Z(N) = \frac{1}{N} [N_c F_{3/2}((F_{1/2}^{-1}(N/N_c)) + N_v F_{3/2}(F_{1/2}^{-1}(N/N_v))] \tag{2.7}$$

with

$$F_j(y) = \frac{1}{\Gamma(j+1)} \int_0^\infty \frac{\xi^j}{1+\exp(\xi - y)} d\xi . \tag{2.8}$$

A parabolic DOS has been assumed. A generalization of (2.6) to more appropriate DOS functions, however, is possible and is given in Appendix A by formula (A4). For the evaluation of (A4), we have chosen two well-known DOS functions: (a) the free-electron DOS, where band tailing is disregarded,

$$g_{\mathrm{parabolic}}(\xi) = \frac{2}{\sqrt{\pi}} \sqrt{\xi} \tag{2.9}$$

and in which case the expression (A4) rewritten in the more familiar Fermi-Dirac integral notation, yields (2.6); (b) the Kane function,[14] taking band tailing into account,

$$g_{\mathrm{Kane}}(\xi) = \frac{2\sqrt{\gamma}}{\pi} \int_0^\infty \exp \left[- \left[t - \frac{\xi}{\gamma} \right]^2 \right] \sqrt{t}\ dt, \tag{2.10}$$

where

$$\gamma = \frac{\sigma}{kT} \tag{2.11}$$

and σ is the mean square of the potential caused by the random distribution of impurities, which is assumed to be Gaussian,

$$\sigma^2 = \frac{q^4}{4\pi\epsilon^2} \frac{N}{\kappa} \tag{2.12}$$

and κ denotes the inverse linear screening length in the Thomas-Fermi approximation. As the doping concentration of the diodes studied lies in the intermediate region, the simple high-density limit screening formula was considered to be inadequate. The general definition in the Thomas-Fermi approach,

$$\kappa^2 = -\frac{q^2}{\epsilon} \int_{-\infty}^{\infty} \rho(\epsilon) \frac{\partial f(\mu)}{\partial \xi} d\xi , \tag{2.13a}$$

where f is the Fermi-Dirac distribution function and μ denotes the Fermi level, or in our $\wp$-transform formalism (see Appendix B)

$$\kappa^2 = \frac{q^2}{\epsilon kT} N_{c\ (v)} \wp \left[\frac{dg_{c\ (v)}}{d\xi}; R_{c\ (v)}^{-1} \left[\frac{N}{N_{c\ (v)}} \right] \right] \tag{2.13b}$$

was calculated self-consistently. For the permittivity in GaAs, we have taken $\epsilon = 13.1\epsilon_0$. The quantity $\Delta V = V_{\mathrm{int}} - E_{g\ \mathrm{av}}$ for the intercept formulas (2.4), (2.5), (2.6), and (A4) invoking (2.10) is drawn in Fig. 2. For low-doping concentrations all studied formula converge, as expected, but divergence occurs when the doping concentration increases. As observed in this plot, an interesting feature of ΔV for sufficiently high doping concentrations, yields

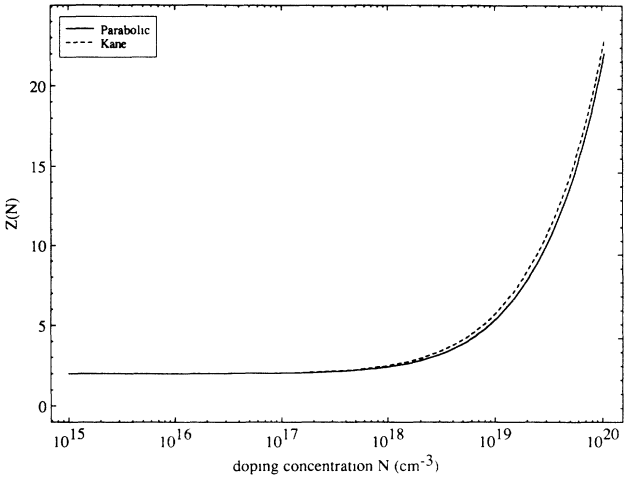

FIG. 1. The function $Z(N)$ [(A5)] calculated for a parabolic DOS, (2.9), and for the Kane DOS, (2.10).

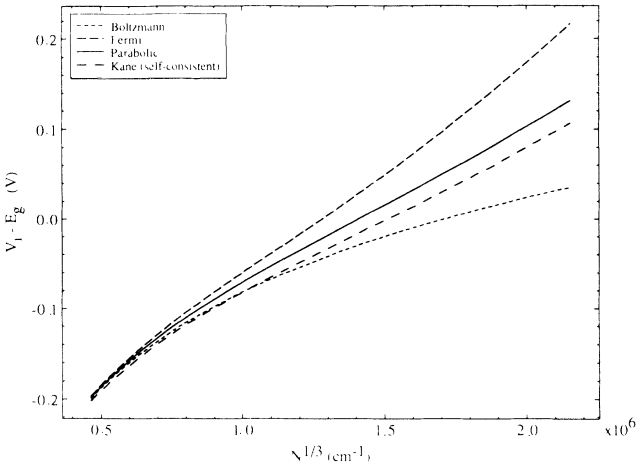

FIG. 2. The quantity $\Delta V = V_i - E_g$ vs doping concentration N to the power $\frac{1}{3}$ calculated for the Boltzmann intercept voltage (2.4), the Fermi intercept voltage (2.5), our intercept voltage for a parabolic DOS (2.6), and for the Kane DOS at room temperature.

$$(\Delta V)_{\text{parabolic}} = O(N^{1/3}) \quad \text{and} \quad (\Delta V)_{\text{Kane}} = O(N^{1/3}) \tag{2.14}$$

while

$$(\Delta V)_{\text{Boltzmann}} = O(\ln(N)) , \tag{2.15}$$

$$(\Delta V)_{\text{Fermi}} = O(N^{2/3}) , \tag{2.16}$$

where O denotes the well-known Bachmann-Landau ("big O") asymptotic notation.

The band-gap narrowing ΔE_g is calculated as

$$\Delta E_g(T) = E_g(T) - E_{g\,\text{av}}(T) , \tag{2.17}$$

where E_g is the band gap of the intrinsic semiconductor which is assumed to obey the Varshni equation[15]

$$E_g(T) = E_g(0) - \frac{\alpha T^2}{T + \beta} \tag{2.18}$$

and for GaAs we have used $E_g(0) = 1.519$ eV, $\alpha = 5.405 \times 10^{-4}$ eV/K, and $\beta = 204$ K. The temperature dependence of $N_{c\,(v)}$ reads

$$N_{c\,(v)} = 2 \left[\frac{2\pi m_0 k}{h^2} \right]^{3/2} (m^*_{c\,(v)} T)^{3/2}$$
$$= 4.829\,30 \times 10^{15} (m^*_{c\,(v)} T)^{3/2} \text{ cm}^{-3} \tag{2.19}$$

(T is expressed in K), where we have taken $m_v^* = 0.572$, and $m_c^* = 0.067$, as advised by Bennett[16] in order to account for the nonparabolicity of the GaAs energy bands, although this nonparabolicity correction does not have a significant effect. Indeed, we have performed the calculations both with these values and the standard parabolic effective masses, $m_v^* = 0.473$ and $m_c^* = 0.067$. For Bennett's values we found, with respect to the standard values, an increasing downward shift in BGN with increasing temperature which never exceeds 5 meV. This number lies within the measurement precision.

III. THE DENSITY OF STATES OF HEAVILY DOPED MATERIAL

Although various DOS functions have been proposed, none of them covers all energies properly. Nevertheless, there are several reasons which justify the use of the proposed functions (2.9) and (2.10).

The choice of the free-electron DOS is evident since it is the most widely used DOS function. In order to take band tailing into account, the Kane function is preferred, because it is the simplest function describing band tailing. Although, the Kane function grossly overestimates the number of deep-tail states at very low energies, this is rather unimportant for this capacitance method, since mainly the majority carriers at both sides of the junction determine the net amount of charges. The deep-tail states contain a negligible amount of particles with respect to the intermediate and high-energy states. We infer therefore, that, in our approach, the precise expression of the exponent in the DOS function for deep tails will have almost no influence on the Fermi level or the total number of particles.[17] This is in contrast with electrical current measurements,[4] where the equilibrium np product is the central quantity to be related to BGN. In this np product, both the majority and minority carriers of the heavily doped region are equally important and for the latter a DOS function, describing deep-tail states properly, should be used as essentially these deep tails are populated.

If deep-tail states are not to be considered here, it is obvious to choose the Kane function. Although this distribution is semiclassical, it is shown[18] that it can be obtained by at least three different methods: the semiclassical method of Bonch-Bruevich, Kane, and Keldysh, the diagram technique of Efros, and the optimum fluctuation method. Moreover, Sa-yakanit and Glyde[19] have compared their Feynman path-integral method with the Halperin and Lax minimum counting method[20] and the Kane function for all energies E, and conclude (see Figs. 6–9 in Ref. 19) that their DOS should be used until it crosses the Kane function and that thereafter for higher energies, the Kane function should be used. This means that the Kane function is the optimal available function for intermediate and high energies. The last reason for choosing (2.9) and (2.10) is that the free-particle DOS overestimates the Fermi level E_F given a fixed number of particles, while the Kane function, as it overestimates tail states, forms a lower bound of E_F. Hence, the obtained values of BGN impose an upper bound (parabolic DOS), and a lower bound (Kane function) for the real BGN.

In the parabolic DOS approximation, both tailing or stretching of the energy states[3] are neglected. In this regard ΔE_g also equals the Fermi-level shift.

IV. EXPERIMENTAL RESULTS

In order to verify the intercept formula (A4) experimentally, diodes in GaAs were grown with a conventional molecular-beam-epitaxial (MBE) process yielding the utmost achievable abruptness. The ratio of the doping

concentrations N_D/N_A was kept as close as possible to 1, as theoretically required,[8] and six symmetrically doped diodes with $N=2.4\times10^{17}$, 6.6×10^{17}, 8.3×10^{17}, 1.2×10^{18}, 1.8×10^{18}, and 2.95×10^{18} cm^{-3} were processed each having the same contact area of 500×500 μm^2. As explained in Ref. 1, higher n (Si) or p (Be) doping is not possible.

The capacitance C was extracted from a measurement of the admittance Y,

$$Y=G+j\omega C\ , \tag{4.1}$$

where $j\equiv\sqrt{-1}$. Since the theory[8] assumes a zero current through the diode, only voltage regions where the conductance G was less than 1 μS were considered. An increasing leakage current for the more highly doped diodes reduces the voltage region and we measured with steps of 0.1 V through the voltage intervals [−4 V, 0.5 V], [−3 V, 0.5 V], [−3 V, 0.5 V], [−2 V, 0.5 V], [−1.5 V, 0.8 V], and [−1 V, 0.8 V], respectively, corresponding to increasing doping concentrations N. Special precautions were taken to outrule external influences on the capacitance measurements. For four of the six diodes, the capacitances were measured at temperatures varying from 77 to 300 K (with a temperature precision of ±1 K). The intercept voltage ($V_{\rm int}$) and effective doping concentration ($N_{\rm eff}$) were deduced from voltage subregions where the correlation coefficient of the straight line fitted through the $C^{-2}(V)$ function was higher than 0.999 99.

In Fig. 3 the majority carrier concentration normalized to the corresponding value at 77 K is drawn on a very sensitive scale. As the absolute accuracy of a concentration is not better than 5%, one may conclude that, in the studied temperature range, the carrier concentration is a very slowly increasing function of temperature and that no carrier freeze-out effect occurs, since its dependence on temperature is exponential.

The influence of an interface charge S reduces the intercept voltage by

$$V_S=\frac{qS^2}{4\epsilon N_{\rm eff}}\ . \tag{4.2}$$

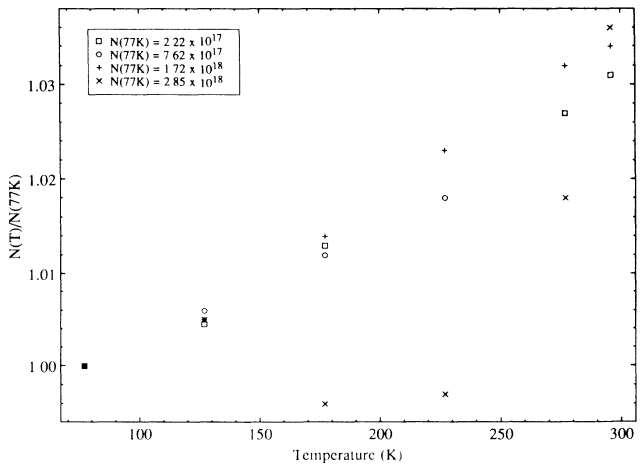

FIG. 3. The majority carrier concentration normalized to the corresponding concentration at 77 K.

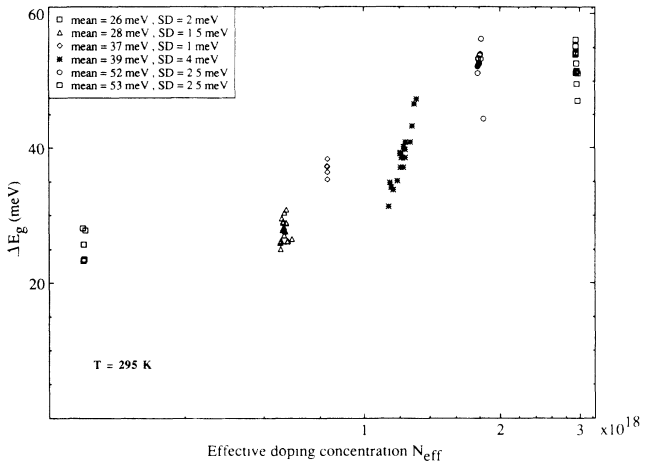

FIG. 4. BGN calculated with (A4) and (2.9) for all measurements at 295 K satisfying the requirements described in the text. SD refers to the standard deviation.

For GaAs pn diodes, grown with MBE, the interface charge S is less than 10^{11} cm^{-2}. For the lowest doping concentration $N=2\times10^{17}$ cm^{-3}, this results in a V_S less than 1.7 mV. Hence, the interface charges do not contribute significantly at all to BGN and consequently, have been neglected.

In order to estimate the accuracy of the method, each measurement at 295 K, satisfying the requirements above and calculated with (A4) using a parabolic DOS (2.9), is shown in Fig. 4. Perfect symmetry is only realizable within 10% (as verified by secondary-ion mass spectroscopy measurements). However, as the area of the device is squared in the calculation of the doping calculation, the inaccuracy on its measurement (due to underetching) outweighs the assumption of perfect symmetry.

V. DISCUSSION

Before discussing the results in detail, a formal consistency of the presented method is given. The mean values of the measured voltage intercepts at 295 K versus the mean values of the effective doping concentrations to the power $\frac{1}{3}$ are plotted in Fig. 5. We find the higher doping concentrations lying on a straight line. From the theoretical calculations of Berggren and Sernelius,[21] it follows that, for high-doping concentrations,

$$\Delta E_g(N)=O(N^{1/3})\ , \tag{5.1}$$

where O denotes the Landau symbol.

Although their calculations were performed for Si and Ge, it is generally agreed and confirmed by experiments (see below) that the same dependence holds for GaAs. Since

$$E_{g\ \rm av}(N)=E_g^{\rm intrinsic}-\Delta E_g(N)$$

we find that

$$V_{\rm int}-E_{g\ \rm av}(N)=O(N^{1/3})\ . \tag{5.2}$$

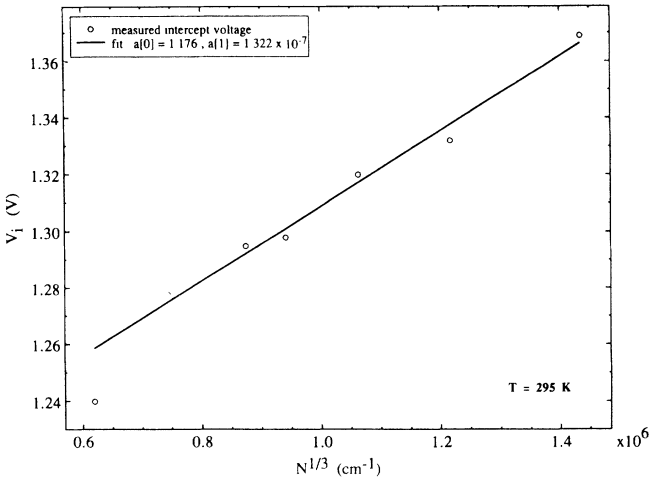

FIG. 5. The mean values of the measured intercept values at 295 K vs the mean values of the effective doping concentration to the power $\frac{1}{3}$. Error bars of ± 5 meV are not shown. The coefficient $a[0]$ is the constant while $a[1]$ equals the slope in the equation of the fitted straight line.

For the doping concentrations considered in Fig. 5, a comparison of (2.14)–(2.16) with (5.2) confirms the superiority of our method (A4).

A. The temperature dependence of ΔE_g

From the measured set $\{V_{\text{int}}(T), N_{\text{eff}}(T)\}$, the band gap narrowing ΔE_g was calculated with the Boltzmann (2.4) and Fermi (2.5) voltage intercept formula, referred to as $\Delta E_{\text{Boltzmann}}, \Delta E_{\text{Fermi}}$, respectively, and with the new formula (A4) for the parabolic DOS (2.9) and for the Kane DOS (2.10), referred to as $\Delta E_{\text{parabolic}}, \Delta E_{\text{Kane}}$, respectively. The results are drawn in Figs. 6–9.

For the lowest doped diode $N = 2 \times 10^{17}$ cm^{-3} (Fig. 9), all BGN values decrease with temperature. For this doping concentration, no experimental temperature-dependent BGN results were found in the literature for GaAs. Lanyon and Tuft[22] have proposed a temperature-dependent ΔE_g formula of the form

$$\Delta E_g = A \frac{q^2}{4\pi\epsilon} \kappa \,, \tag{5.3}$$

where κ is the inverse screening length (2.13) and $A_{\text{LT}} = 0.75$. Although Mahan[23] has rejected this theory for several reasons, this term (with $A_{\text{Inkson}} = 1$) also appears in the Inkson model.[24] Moreover, Landsbergh *et al.*[25] find a good agreement between (5.3) with $A_{\text{Landsbergh}} = 1$ and experimental results of various authors in Si. Relying on these arguments and merely guided by the simplicity of the expression (5.3), it gave us a suggestion to fit our results with

$$\Delta E_g = A \frac{q^2}{4\pi\epsilon} (\kappa_n + \kappa_p) \,, \tag{5.4}$$

where $\kappa_{n\,(p)}$ is the inverse Thomas-Fermi screening length in n-type (p-type) material. The results are shown in Fig. 9 for both a parabolic and Kane DOS in (2.13). For this doping concentration, an inverse square-root dependence

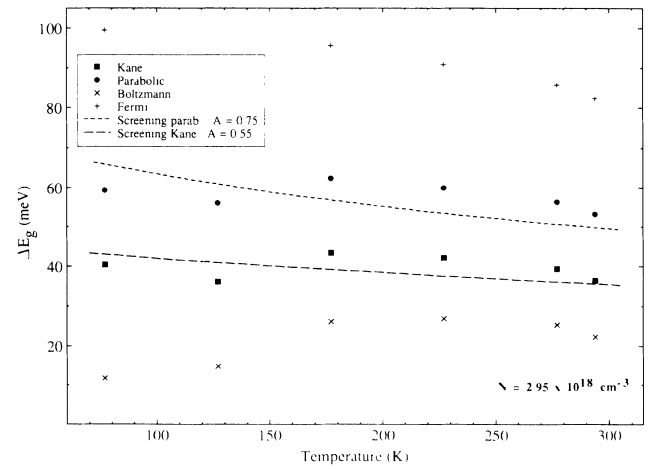

FIG. 6. BGN vs temperature for effective doping concentration $N = 2.95 \times 10^{18}$ cm^{-3}. Also $\Delta E_{\text{Boltzmann}}$ and ΔE_{Fermi} (not drawn in Figs. 7–9 for clarity) are shown. Notice the slow increase with temperature and the too low values of $\Delta E_{\text{Boltzmann}}$ while ΔE_{Fermi} exaggerates BGN.

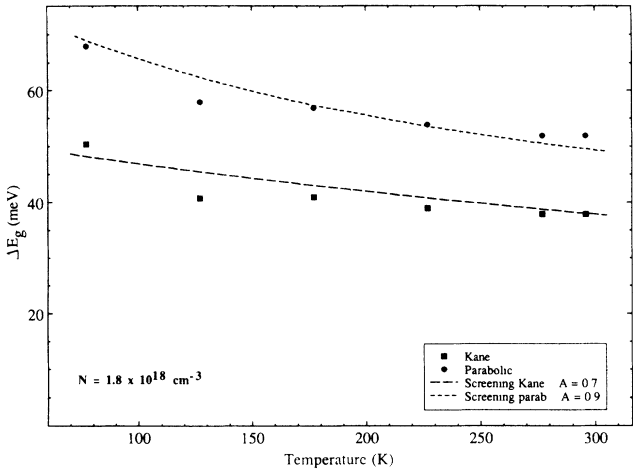

FIG. 7. BGN vs temperature for $N = 1.8 \times 10^{18}$ cm^{-3}.

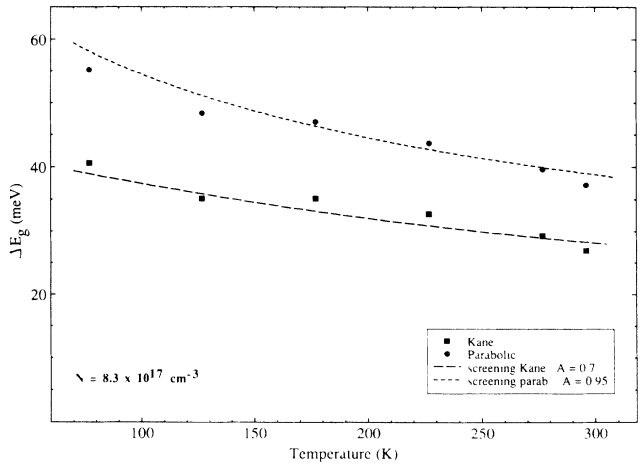

FIG. 8. BGN vs temperature for $N = 8.3 \times 10^{17}$ cm^{-3}.

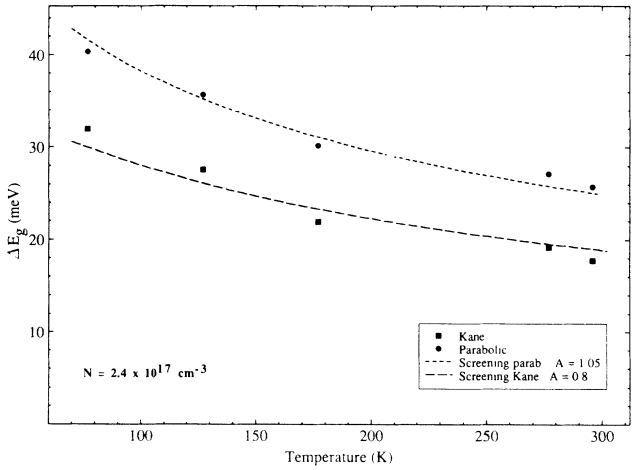

FIG. 9. BGN vs temperature for $N=2.4\times10^{17}$ cm^{-3}.

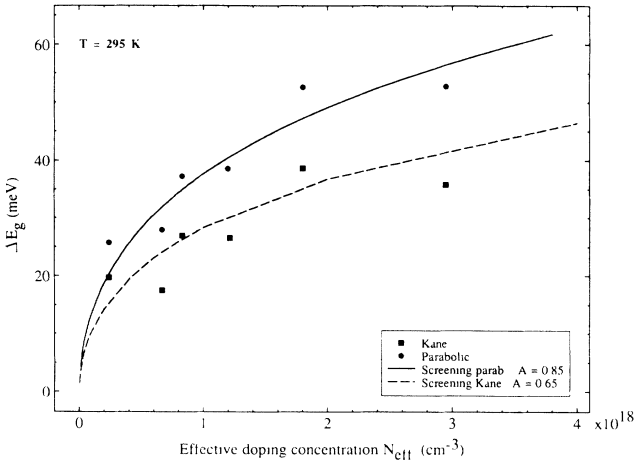

FIG. 10. BGN at 295 K vs effective doping concentration. The data are fitted with (5.4) for both a parabolic DOS and the Kane DOS.

of BGN on temperature is found. Abram *et al.* have given a temperature-dependent BGN formula [(3.21) in Ref. (26)] using both the Thomas-Fermi approach and the Boltzmann statistics, which includes besides screening effects (5.3), also an exchange contribution. The latter, however, follows a rather complicated temperature dependence, which is obviously not seen. For nondegenerate materials, this confirms the BGN theory[26] which states that screening is the dominant process.

For the higher doping concentrations $N=1.8\times10^{18}$ cm^{-3} and 2.9×10^{18} cm^{-3} (Figs. 6 and 7), the change of $\Delta E_{\text{parabolic}}$ and ΔE_{Kane} with temperature, within the measurement precision, is zero. This is in perfect agreement with the PL measurements of Olego and Cardona.[27] For the intermediate doping concentration, ΔE_g (Fig. 8) clearly lies between the two regimes described above.

In spite of the good temperature fitting of the $\Delta E_{\text{parabolic}}$ and ΔE_{Kane} values with (5.4), there are several reasons why (5.4) can be criticized. First of all, we note the main objection of Mahan[23] that (5.3) only describes one BGN phenomena and neglects, besides anisotropy and intervalley scattering, exchange effects. Secondly, we used the Thomas-Fermi approach for simplicity. This high-density limit theory overestimates, the BGN as shown by Abram *et al.*[26] Further, ΔE_{gp} calculated with (5.3) turns out to be always greater than ΔE_{gn} because κ_p is always greater than κ_n. However, just the opposite is found in both experiment[1] and theory.[3,28] For the doping concentrations studied, we infer that (2.13) only gives an order of magnitude and that a more accurate screening model together with the exchange contribution should be used. Although the results of Berggren and Sernelius[21] can be extended to a temperature-dependent Green's function formalism, the numerical evaluation lies beyond the scope of this paper.

B. The doping concentration dependence of ΔE_g

The set of ΔE_g values at 295 K versus doping concentration together with fits of (5.4) for both the Kane and parabolic DOS is shown in Fig. 10, while in Fig. 11 $\Delta E_{\text{parabolic}}$ and ΔE_{Kane} versus $N^{1/3}$ are plotted.

The $\Delta E_{\text{parabolic}}$ and ΔE_{Kane} obey the $\frac{1}{3}$ power law[21] very well (Fig. 11), or

$$\Delta E_{\text{parabolic}}=B_{\text{parabolic}}(N_{\text{eff}})^{1/3},$$

with

$$B_{\text{parabolic}}=3.76\times10^{-5}\ \text{meV cm}, \tag{5.5}$$

and

$$\Delta E_{\text{Kane}}=B_{\text{Kane}}(N_{\text{eff}})^{1/3},$$

with

$$B_{\text{Kane}}=2.64\times10^{-5}\ \text{meV cm}. \tag{5.6}$$

The values of the coefficient B in (5.5) and (5.6) are in good agreement with optical measurements. Casey and Stern[29] extracted only for p-type material a coefficient $B_p=1.6\times10^{-5}$. Borghs *et al.*[1] have extracted both the Fermi-level shift ΔE_F and the band-gap narrowing ΔE_g

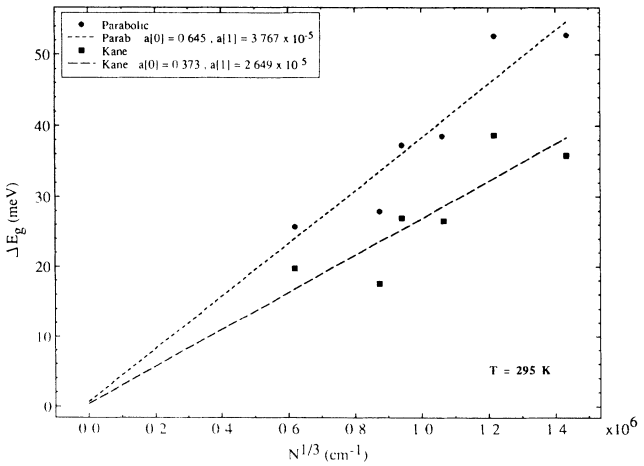

FIG. 11. BGN calculated with (A4) using (2.9) and (2.10) at 295 K vs effective doping concentration to the power $\frac{1}{3}$. The coefficient $a[0]$ is the constant, while $a[1]$ equals the slope in the equation of the fitted straight line.

for both p-type and n-type material. Since their values for the Fermi level are calculated in the assumption of a parabolic band, their values are higher than in the case of a tailed distribution, as explained in Sec. III. Due to lifetime-broadening effects,[28] which trouble the low-energy PL spectrum and which cause a certain restriction for optical models, the extrapolated values of ΔE_g are less accurate. However, if one takes their ΔE_F values for the ΔE_g and if one uses also a parabolic DOS, one notices a very nice agreement between $B_{\text{parabolic}}$, (5.5), and the average of their $B_n = 4.6\times10^{-5}$ and $B_p = 2.6\times10^{-5}$. This justifies the assumption (2.3).

The comparison between the theoretical results of Bennett and Lowney[30] is difficult to accomplish since their Figs. 12 and 13 do not give the values of the p type for our relatively low-doping concentrations.

VI. CONCLUSION

A new analytical intercept voltage formula is employed to interpret the BGN from capacitance data of a symmetrical abrupt diode. The average BGN of GaAs is obtained for a doping range from 2×10^{17} to 3×10^{18} cm^{-3} for various temperatures and compared to values obtained by optical measurements. A good agreement is found and the quality of the proposed formula is demonstrated.

The experimental accuracy of ±5 meV, the not substantial difference between results obtained by (2.9) and (2.10), and the fact that both used DOS functions form limits between which the real ΔE_g lies, suggest that in calculations (e.g., device simulators) a parabolic DOS may be employed to reduce computational efforts.

ACKNOWLEDGMENTS

The authors thank D. Uwaerts for his help with the installation of the precision capacitance measurement configuration.

APPENDIX A: THE INTERCEPT VOLTAGE FORMULA OF AN ABRUPT JUNCTION

In our study of the capacitance of an abrupt diode,[8] an analytical formula for the low injection regime is both derived and discussed. In order to account for an arbitrary DOS function, a new transformation is created which is briefly resumed in Appendix B.

For symmetrical junctions ($N_D = N_A = N$), the capacitance formula inverse squared as a function of the applied voltage V, reads

$$C^{-2} = \frac{4}{q\epsilon N}\left[-V + \frac{E_{gn}+E_{gp}}{2} + \frac{kT}{q}u_B\right] \tag{A1}$$

where

$$u_B = R_v^{-1}(N/N_v) + R_c^{-1}(N/N_c) - \frac{N_c}{N}\mathcal{J}_c(R_c^{-1}(N/N_c)) - \frac{N_v}{N}\mathcal{J}_v(R_v^{-1}(N/N_v)) \; . \tag{A2}$$

The slope is given by

$$\frac{dC^{-2}}{dV} = -\frac{4}{q\epsilon N} \; . \tag{A3}$$

This is in complete agreement with the classical formula.[13] Formula (A3) offers an accurate method to extract the doping concentration N from capacitance measurements.

The voltage intercept V_{int} is defined as the asymptotic voltage for which $C^{-2}(V)=0$. This quantity has no physical meaning (as there exists no such voltage in reality) and can only be obtained by extrapolation of capacitance values from the low injection region. Using the $C^{-2}(V)$ relation (A1) and the notation of (2.3), the voltage intercept V_{int} is

$$V_{\text{int}} = E_{g\,\text{av}} + \frac{kT}{q}[R_c^{-1}(N/N_c) + R_v^{-1}(N/N_v) - Z(N)] \tag{A4}$$

while

$$Z(N) r \frac{N_c}{N}\mathcal{J}_c(R_c^{-1}(N/N_c)) + \frac{N_v}{N}\mathcal{J}_v(R_v^{-1}(N/N_v)) \; . \tag{A5}$$

This voltage intercept (A4) can be expressed as an integral,

$$V_{\text{int}} = E_{g\,\text{av}} + \frac{kT}{q}\left[\frac{1}{N}\int_0^N [R_c^{-1}(\zeta/N_c) + R_v^{-1}(\zeta/N_v)]d\zeta\right] . \tag{A6}$$

The capacitance C was simulated with SEDAN3[31] for $N_D = N_A = N$ and $E_{g\,p\text{GaAs}} = E_{g\,n\text{GaAs}} = E_g = 1.424$ V (300 K). The voltage range was $[-15$ V,0 V] in steps of 0.1 V. The results were reformed into a $C^{-2}(V)$ graph. By linear regression, V_{int} was obtained. In contrast with the formulas (2.4) and (2.5), a perfect matching of these values with our analytical formula (A4) [with $g_c = g_v = (2/\sqrt{\pi})\sqrt{\xi}$], was found.

APPENDIX B: THE $\wp$ TRANSFORMATION

In this appendix, symbols used in our $\wp$ transformation formalism are given. The properties of the $\wp$ transformation are listed in our theoretical paper.[8]

The $\wp$ transformation of a function $f(\xi)$ is defined as

$$\wp(f(\xi),y) = \int_{-\infty}^{\infty} \frac{f(\xi)}{1+\exp(\xi-y)}d\xi \tag{B1}$$

and we call

$$R_c(y) = \wp(g_c(\xi),y) \; , \tag{B2}$$

where $g_c(\xi)$ is related to the DOS in the conduction band ρ_c by

$$g_c(\xi) = \frac{kT}{N_c}\rho_c(kT\xi) \; , \tag{B3}$$

where $\xi = (E - E_c)/kT$ and E_c is the unperturbed or

mean (equivalent to E_0 in Refs. 19 and 20) band edge. The inverse function $R^{-1}(z)$ is defined as

$$\forall z,y \in \mathcal{R}: \; z = R(y) \Longleftrightarrow y = R^{-1}(z) \; . \tag{B4}$$

Finally, we denote

$$\mathcal{J}_c(y) = \wp \left[\int_{-\infty}^{\xi} g_c(\tau) d\tau, y \right] \; . \tag{B5}$$

[1]G. Borghs, K. Bhattacharyya, K. Deneffe, P. Van Mieghem, and R. Mertens, J. Appl. Phys. **66**, 4381 (1989).

[2]See, for example, J. I. Pankove, J. Appl. Phys. **39**, 5368 (1968).

[3]See, for example, Bo E. Sernelius, Phys. Rev. B **33**, 8582 (1986).

[4]See, for a review, R. P. Mertens, R. J. Van Overstraeten, and H. J. De Man, *Advances in Electronics and Electron Physics* (Academic, New York, 1981), Vol. 55, p. 77.

[5]S. T. Pantelides, A. Selloni, and R. Car, Solid State Electron. **28**, 17 (1985).

[6]H. S. Bennett, Solid State Electron. **28**, 193 (1985).

[7]J. Del Alamo, S. Swirhun, and R. M. Swanson, Solid State Electron. **28**, 47 (1985).

[8]P. Van Mieghem, R. P. Mertens, and R. J. Van Overstraeten, J. Appl. Phys. (to be published).

[9]R. J. Van Overstraeten, H. J. De Man, and R. P. Mertens, IEEE Trans. Electron Dev. **ED-20**, 290 (1973).

[10]M. E. Klausmeier-Brown, M. S. Lundstrom, M. R. Melloch, and S. P. Tobin, Appl. Phys. Lett. **52**, 2255 (1988).

[11]J. R. Lowney, Solid State Electron. **28**, 187 (1985).

[12]B. R. Chawla and H. K. Gummel, IEEE Trans. Electron Dev. **ED-18**, 178 (1985).

[13]S. M. Sze, *Physics of Semiconductor Devices* (Wiley, New York, 1981), p. 74.

[14]E. O. Kane, Phys. Rev. **131**, 79 (1963).

[15]Y. P. Varshni, Physica (Utrecht) **39**, 149 (1967).

[16]H. S. Bennett, J. Appl. Phys. **60**, 2866 (1986).

[17]C. J. Hwang, J. Appl. Phys. **41**, 2668 (1970).

[18]B. I. Shklovskii and A. L. Efros, *Electronic Properties of Doped Semiconductors* (Springer-Verlag, Berlin, 1984), Pt. II, pp. 255–293.

[19]V. Sa-yakanit and H. R. Glyde, Phys. Rev. B **22**, 6222 (1980).

[20]B. I. Halperin and M. Lax, Phys. Rev. **148**, 722 (1966); **153**, 802 (1967).

[21]K. F. Berggren and B. E. Sernelius, Phys. Rev. B **24**, 1971 (1981).

[22]H. P. D. Lanyon and R. A. Tuft, IEEE Trans. Electron Dev. **ED-26**, 1014 (1979).

[23]G. D. Mahan, J. Appl. Phys. **51**, 2634 (1980).

[24]J. C. Inkson, J. Phys. C **9**, 1177 (1976).

[25]P. T. Landsberg, A. Neugroshel, F. A. Lindholm, and C. T. Sah, Phys. Status Solidi B **180**, 255 (1985).

[26]R. A. Abram, G. J. Rees, and B. L. H. Wilson, Adv. Phys. **27**, 799 (1978).

[27]D. Olego and M. Cardona, Phys. Rev. B **22**, 886 (1980).

[28]Bo E. Sernelius, Phys. Rev. B **34**, 5610 (1986).

[29]H. C. Casey and Frank Stern, J. Appl. Phys. **47**, 631 (1976).

[30]H. S. Bennett ad J. R. Lowney, J. Appl. Phys. **62**, 521 (1987).

[31]Z. Yu and R. W. Dutton, SEDAN III, a generalized electronic material device analysis program, Integrated Circuits Laboratory, Stanford University (1985) (unpublished).